EXPERIMENTAL INVESTIGATIONS OF INJECTION AND COMBUSTION PARAMETERS OF A HOMOGENEOUS CHARGE COMPRESSION IGNITION (HCCI) ENGINE WITH A MULTI-INJECTION COMMON RAIL SYSTEM

Waleed Niklawy[1], Moatasem Shahin[2], Mohamed I. Amin[1,*], Ali Elmaihy[1]

[1]Mechanical Power Engineering Department, Military Technical College, Cairo, Egypt
[2]Mechanical Engineering Department, School of Engineering, Badr University in Cairo, Cairo, Egypt

*E-mail of corresponding author: mamin@mtc.edu.eg

Resume

This work experimentally investigates the most imperative parameters that control the injection and combustion processes in a multi-injection HCCI Diesel engine namely; fuel-line pressure, timing of multi-injection events and the resulting in-cylinder pressure. These parameters in addition to the heat release rates are evaluated at different engine loads and speeds over up to 42 successive cycles. The main inter-relations of these parameters are also discussed.

Results revealed that the maximum cylinder pressure and temperature in the HCCI engines are lower by 7% compared to similar conventional ones, which could lead to lower NOx emission. In addition, the fuel line pressure exhibits nearly the same major frequency of the waves, 850 to 950 Hz. Those results could be very useful for engine assessment, modeling, control, NO_x reduction and power saving.

Article info

Received 4 August 2021
Accepted 16 November 2021
Online 21 January 2022

Keywords:

HCCI
fuel line pressure
AHRR
injector activation signals
multi-injections CR system

Available online: https://doi.org/10.26552/com.C.2022.2.B120-B134

ISSN 1335-4205 (print version)
ISSN 2585-7878 (online version)

1 Introduction

Recently, an alternative combustion technology that has the potential to decrease emissions and fuel consumption has emerged. This newly introduced technology is known as Homogeneous Charge Compression Ignition (HCCI). The main concept of the HCCI is to combine the high compression ratio and efficiency of the diesel engine with the tailpipe emission levels of spark-ignition engines since the admitted charge is a lean mixture prepared either externally or internally [1-2]. However, controlling the HCCI auto-ignition timing and rate of the heat release, at all operating regimes, presents the biggest challenge due to the complicated and highly coupled combustion problems [3]. Tackling these challenges in the HCCI diesel engines becomes possible after the successful implementation of the high-pressure common rail (CR) injection system and fast response electro-hydraulic injectors, which are capable to optimize the injection parameters, at high fuel pressure, provide the high precision of the injected fuel volume and realize multi injections in a very short duration [4-5].

Auto-ignition of the HCCI combustion is fully controlled by Chemical kinetics. It is directly affected by engine operating conditions (load, speed, etc.), boundary conditions (environmental temperature, pressure and humidity), and the chemical composition of used fuel (ratio and thermodynamic state of the fuel-air mixture) [6-8]. So, fuel-line pressure, the timing of multi-injection events and the resulting in-cylinder pressure data, over the entire operating regimes, are of a great importance for the assessment of the engine combustion process, which is the foundation of simultaneous engine performance enhancement with lower emission levels. These data are also very beneficial for developing and verifying mathematical models for the injection system and combustion process. Thus, intensive experimental analysis of engine performance parameters is mandatory.

In fuel lines, the pressure fluctuations at the injector inlets, due to injector nozzle opening and closing, are intrinsic difficulties in common rail systems [9-11]. These fluctuations produced by an initial injection may still be present when the injector is reopened in multiple injection strategies. This gives an unquantified effect on the amount of fuel injected, spray atomization, penetration and mixing of the injected fuel with air. These pressure variations also affect the injector function and modify the needle lift level [12]. Different mechanisms for fluctuating fuel pressure and deviating fuel mass were historically studied. High-pressure fuel pipe sizes and relative dimensions have a significant influence on

fluctuation of the fuel pressure [13-14]. Results showed that amplitude reduction and frequency increase of the pressure wave can be attained by decreasing the length and increasing the inner diameter of the injector high-pressure supply pipe. The effect of the fuel properties on the pressure fluctuation of a common rail fuel line was investigated in [15]. Henein et al. [16] studied the effect of pressure fluctuation on the injector needle left and subsequently the fuel-injected quantity. The effects of common rail pressure and injection pulse width were studied in [17-18]. Some investigations were conducted to assess the mechanisms by which the amplitude of multi-injection fuel mass deviation can be significantly reduced [19-20]. The impact of the pilot pressure parameters on the fuel line pressure pulsation was studied by [21-23].

In multi-injection events, the number of injections, Start of Injection (SOI), Energizing Time (ET), Dwell Time (DT) and the rail pressure are the most important parameters related to the engine injection system and greatly affect the combustion phasing and efficiency, emissions and performance characteristics of HCCI engines [24-25]. These are also very important input parameters for injection systems and combustion process modeling, assessment and control [26]. The electric current signal profile controlling the operation of the injector is a signature but not the same as the injection rate profile. There is a time delay between the start of the controlling electric signal and the start of the injection [26], as well as a time delay between the start of injection and the start of combustion (SOC). Electronically controlled fuel injection system is capable of changing the common rail pressure, the injection pressure and allows for flexible injection timings with accurate control of the injection quantity and pattern as a function of the engine speed and torque [27]. Thus, the engine injection system should be capable of managing multiple injection strategies in order to accomplish painstaking fuel-air mixing and evade wall wetting [28-29]. Wanhua et al. [30] found that, for early injections, short pulse widths should be used to provide enhanced evaporation and mixing rate, while for late injections, short DTs result in more homogeneous fuel to air mixture. The injected fuel quantity ratio among pulses and the number of injection pulses were defined as critical aspects in the HCCI injection operation [31]. The dynamic response of the fuel injection system was investigated in the case of multiple injections for different values of energizing time (ET) nominal rail pressure and dwell time, (DT) [32]. It is, therefore, necessary for the HCCI engine assessment, modeling and control, to investigate SOI, EI, DT and their relationship with in-cylinder and fuel line pressure at different deriving modes, i.e. different speeds and loads.

In-cylinder pressure recording can be considered as the most reliable method of obtaining information about the ICE combustion processes such as load (IMEP), heat release (HR) characteristics and ringing. Distinguishing the early stages of HR, the timing of the main HR and maximum heat release rate (HRR) are crucial for achieving any control scheme for the HCCI combustion engine. The literature includes a few performed works specifically on the HR performance in the HCCI engines at different design and operational engine parameters. The effect of different locations and voltage supplied of controlled glow plug on HRR of HCCI engine was studied by [33]. The effect of combustion phasing, intake temperature, equivalence ratio and load, on the combustion performance of HCCI engines have been studied by Lawler in [34]. Ebrahimi et al. [35] carried out experimental research on the effect of two engine speeds (600 and 900 rpm) for different equivalence ratios (0.1 to 0.38) on HCCI engine combustion parameters derived from the AHRR gained during a cycle from the first thermodynamics principle.

The previous literature survey exhibits obvious gaps that should be covered in order to reveal the ambiguity and assists in deep understanding. None of the previous works introduced coincident comprehensive measurement and analysis for the fuel line pressure, injector activation signal, in-cylinder pressure and AHHR in addition to their mutual effects for the same engine at different engine speeds and loads over the entire operating range of the engine.

This paper addresses the most imperative parameters that control combustion in an HCCI diesel engine. The objective of this paper is to experimentally analyze fuel line pressure data (average value and frequency) and in-cylinder pressure (maximum value, history and AHRR). These analyses, with the aid of measuring the injector activation signals, could be very useful for developing injection system and combustion models, engine performance assessment and control, which lead to power saving and emission reduction.

2 The test facility

A 4-stroke, 4-cylinder, 2.776 liter water-cooled compression ignition engine with overhead valve mechanism was used. The main engine design parameters are listed in Table 1. The engine is turbocharged and the compressed air is cooled before entering the intake manifold. The fresh charge is internally prepared by injecting fuel twice, the first just before and the second just after the Top Dead Center (TDC) before the suction stroke. This early injection, using the same high-pressure CR injection system, allows for fuel heating and distribution, which gives more time for fuel vaporization and mixing with air [36]. Combustion is triggered by a pilot injection, just before the Top Dead Center (TDC), followed by a secondary (main) injection, typically starting at the TDC. In-cylinder pressure, fuel line pressure and injector triggering signals are measured at different speeds and loads using the test bench schematically shown in Figure 1.

Table 1 *Engine specifications*

Description	Specification
Engine type	R2816K5A
Bore	94 mm
Stroke	100 mm
weight	270 kg
Compression Ratio	17.5
Number of Cylinders	4
Displacement	2776 cc
Max power	90 kW (120H.P.) @ 3800 RPM
Peak Torque	400 N·m (295 ft.lb.) @ 1800 RPM
Fuel primary pump	Electric pump
Fuel System	Direct Fuel Injection Common Rail System
High-Pressure Fuel Pump	Radial Piston Pump (3 pistons)
Injection pump	CP3 2nd Generation Common Rail
Timing System	Valve Belt Driven DOHC Overhead Camshafts

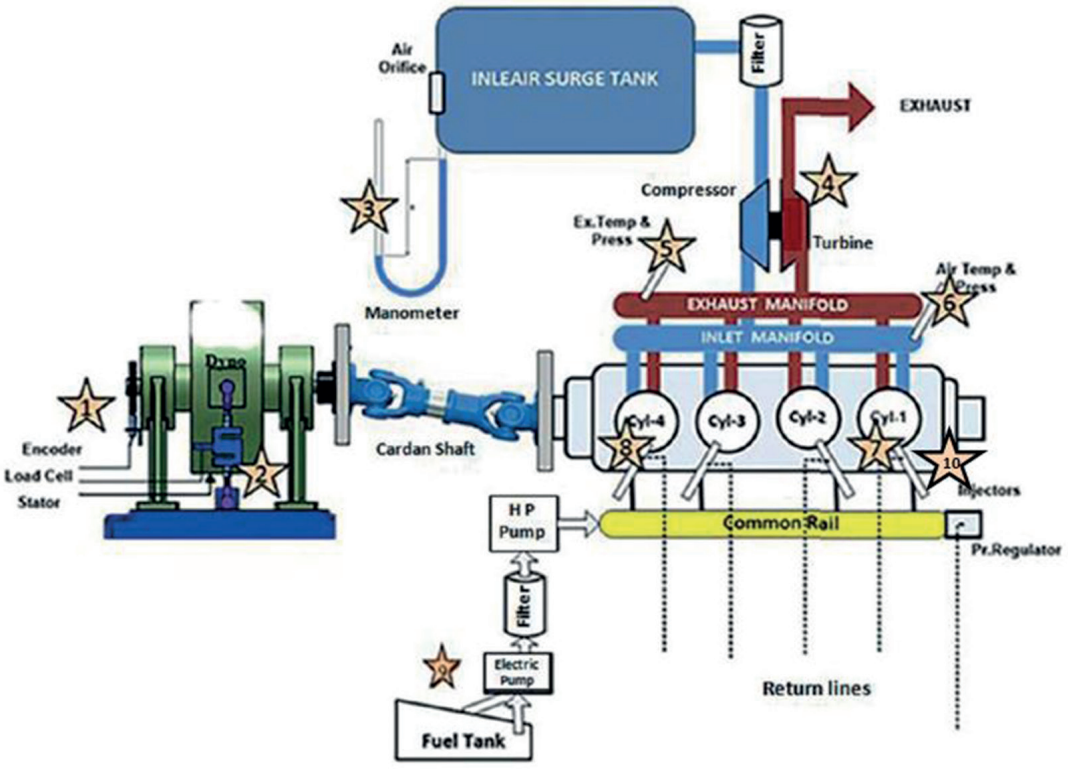

Figure 1 *Schematic of the engine test facility, measured parameter numbers and locations*

The main measured parameters are marked in Figure 1 and listed in Table 2.

Engine external loading is carried out by an ELZE /Heenan water dynamometer (Type AN5F), with maximum braking power of 170 kW at 4000 rpm. The S-type load cell (strain gauge) is inserted under the dynamometer torque reaction arm. The load cell output signal is amplified and fed to the data acquisition interface.

2.1 Cylinder pressure measurement

A water-cooled piezoelectric transducer, (type PCB model no. 112B11) with range (3: 20685 kPa), resolution (0.069 kPa), sensitivity (0.145 pC/kPa) and resonant frequency (≥ 200 kHz) is used for measuring cylinder pressure. The used charge amplifier is a PCB type, with the capability of statically holding the output charge for calibration processes. Errors due to output

drift, during dynamic operation, are minimized by keeping all electric connections spotlessly clean, cables shielding and limiting the test duration. The transducer is mounted on the cylinder head above cylinder no. 1 where suitable and enough space could be found.

2.2 Fuel line pressure sensor

A piezoelectric transducer type (Kistler PN 6278) and charge amplifier (Kistler SN 284625) are used to measure the fuel line pressure. This setup is capable of measuring pressure up to 3000 bars. The transducer, amplifier and cabling were calibrated together using a deadweight tester.

2.3 Injector trigger signals

A dual-channel GwIntek oscilloscope GO-635, 35 MH is used to display the injector triggering signals for confirmation. The signal has been acquired digitally for recording and further analysis using a 12-bit analog to digital National Instruments data acquisition card (PCI-MIO-16E-1).

2.4 Crank-angle and engine speed

An incremental digital quadrature encoder (type WDG 58B-360-ABN-G24-K3) is used for engine speed measurement. The encoder gives 2 trains of pulses (A and B), each has 360 pulses per encoder shaft revolution (360 ° Crank angle CA). The two trains are phased by ¼ pulse and a third index train (N) with one pulse per each revolution is also produced. The encoder output pulses are fed to the data acquisition interface, where pulses A and B are used as the timer sampling events. The index pulse (N) is used to synchronize the start of measurement with the TDC of cylinder 1. The frequency of output pulses A or B is measured and used to calculate the engine speed with the utmost accuracy.

2.5 Data acquisition system

The data acquisition system is a PC-based card and a personal computer (PC) with the appropriate software. The card is used to collect the signal (analog or digital) from the measuring instruments through a BNC panel. Measurements are then converted to digital data and recorded by the PC under software control. The BNC connector is National Instrument panel BNC-2120. Analog and digital inputs are connected to the BNC panel, which relays all signals to the data acquisition card through a special 68-pin cable.

A National Instruments data acquisition card (PCI-MIO-16E-1) is used. This is a 12-bit, 16 analog input channels, 16 digital I/O ports and two 24-bit general-purpose timers/counters. This card is capable of reading signals at a total frequency of 1.25 Mega samples per second, which is more than adequate for engine measurement purposes.

The computer data acquisition software has been developed in Visual Basic to automate the measuring, recording and processing of measurements. The software is adjusted to acquire up to 8 differential signals with different resolutions, offset and calibration constants. Fast-changing parameters, such as in-cylinder and fuel line pressures, are measured at high frequency (at least every one degree of crank angle rotation). Other slow-changing parameters (engine speed and load) are measured at regular intervals, typically 0.1 sec.

3 Results and analysis

Fast-changing parameters, such as in-cylinder and fuel line pressures, are averaged at each crank angle over several successive engine cycles. The coefficient of variance (COV) for the considered successive cycles (typically from 10 to 42) is then evaluated in an ascending way until a steady value is obtained. Data analyses show that the COV becomes steady after 20 cycles within ± 2% for in-cylinder pressure and ±3% for fuel line pressure, which are comparable to [37-39]. This confirms the validity of the acquired data and its suitability for further calculations.

The computation of the uncertainty for measuring instruments is carried out according to [40]

$$\Delta x_i = \left(\frac{2\sigma}{\overline{X}_l}\right), \tag{1}$$

where, Δx_i = uncertainty, σ = standard deviation, $\overline{X}_l$ = mean value.

The uncertainty calculations for every measuring device are shown in Table 2.

Figure 2 shows an example of the changes in the measured parameters with crank angle during a complete cycle at constant engine speed and load.

3.1 Fuel line pressure

The effect of engine speed and load on the amplitude of fuel line pressure wave was studied by the authors [41]. The mean value of common rail pressure is the result of the high-pressure fuel pump characteristics and the flow requirements of the injection system (piping characteristics) at any engine speed for different pressure control valve energizing times (ET). Each piping characteristic affects the overall amount of fuel expelled by the four electro-injectors depending on the common rail pressure and the injector energizing duration [42]. The mean value of the pressure is found to

Table 2 *A list of measured parameters, the corresponding locations relevant to Figure 1, their accuracy and uncertainty*

Meas. point no.	Measured Parameter	Instrument	Range	Accuracy	Uncertainty %
1	Incremental Encoder, Engine Speed and Crank Angle	Encoder Incremental (WD GI 58B)	1 pulse / 0.25 ^{O} CA to 1 pulse / 1 ^{O} CA	Phase Shift 90° ± max. 7.5% of the period duration pulse-/ pause-ratio ≤ 5000 ppr: 50% ± max. 7%	± 0.6
2	Load Cell, Engine Torque	S-type load cell	Up to 500 kg	Combined error < 1%	± 0.1
7	Cylinder Pressure	piezoelectric transducer type PCB (model no. 112B11)	0.03-206 bar	< 0.6% FS ± 1.25 bar FS	± 0.2
8	Injector Line Pressure	piezoelectric transducer type (Kistler PN 6278)	up to 3000 bars	< 0.2% FS 6 bar FS	± 0.3
10	Injector triggering signals	GwIntek oscilloscope GO-635. 35 MH	35 MHz	5 mV ~ 5 V/div 4%	± 0.5

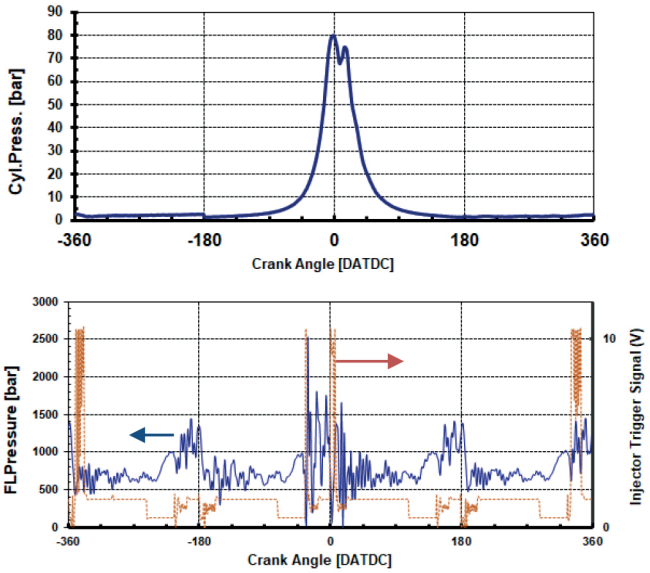

Figure 2 *Example of the fast-changing parameters with the crank angle during a complete cycle at speed of 2003 rpm and torque of 206.45 N.m*

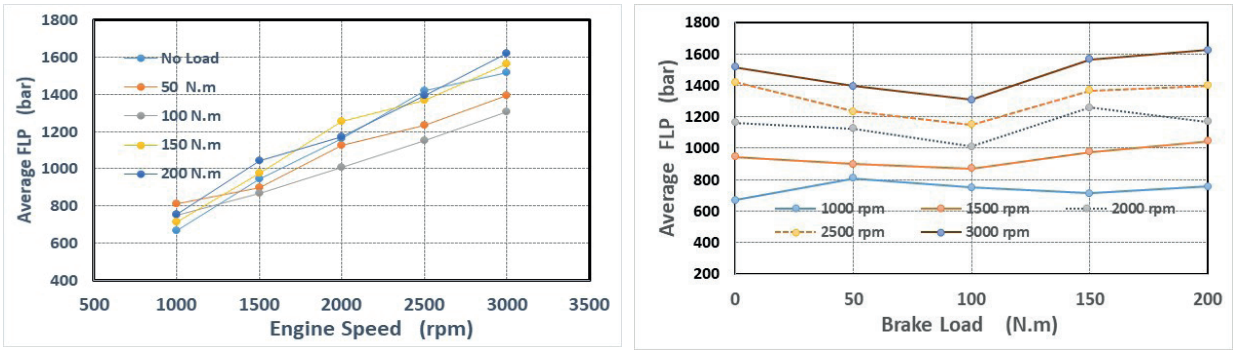

a) At constant brake loads *b) At constant speeds*

Figure 3 *Average fuel line pressure*

increase with engine speed and marginally with load, as shown in Figure 3. Typically, at 3000 rpm, the average value of fuel line pressure increased from 1408 bar at 50 N.m brake load to 1584 bar at 150 N.m then increased

to 1610 bar at 200 N.m. For engine load of 200 N.m, the average value is found to increase from 750 bar at 1000 rpm to 1150 bar at 2000 rpm to 1610 bar at 3000 rpm.

The repeated pattern of FLP variation at different operating conditions suggests that the pressure waves traveling along the fuel line have almost similar characteristics. The fast Fourier transform (FFT) of the FLP is carried out and presented in Figure 4. It is found that in all cases, a major frequency is observed at the frequency 850 to 950 Hz. The speed of the pressure wave is calculated from [12]:

$$c = \sqrt{\frac{B_{fuel}}{\rho_{fuel}}}\,. \tag{2}$$

If Bulks modulus of the fuel B_{fuel} is assumed between $1.4\text{x}10^9$ to $2\text{x}10^9$ Pa, (typically $1.7\text{x}10^9$) and the diesel fuel density, ρ_{fuel} is 850 kg/m^3, the wave speed would then be 1440 m/sec. The fundamental frequency of a closed-open boundary system is calculated from the length of the pipe, l and the speed of the pressure wave, c and is given as [12]:

$$f_{closed-open} = \frac{c}{4 \times l}\,. \tag{3}$$

The pipe length required to reflect the pressure wave with this frequency should be nearly 0.38 to 0.43 m. The length of the high-pressure fuel line between the fuel pump and the injector inlet was found to be 0.395 m, which confirmed the observation. Similar observations were reported earlier [12] with almost the same dominant frequency of 850 Hz at 1600 rpm and 4.39 bar BMEP. Baumann et al. [17] reported a value of 850 Hz using Magneto-Elastic Sensors. They concluded that with such information it is possible to estimate the influence of pressure waves on neighboring injections.

3.2 Injector trigger signals

The Electronic Control Unit (ECU) activates each fuel injector 4 times per cycle. A fraction of the fuel is first injected into the cylinder before the compression

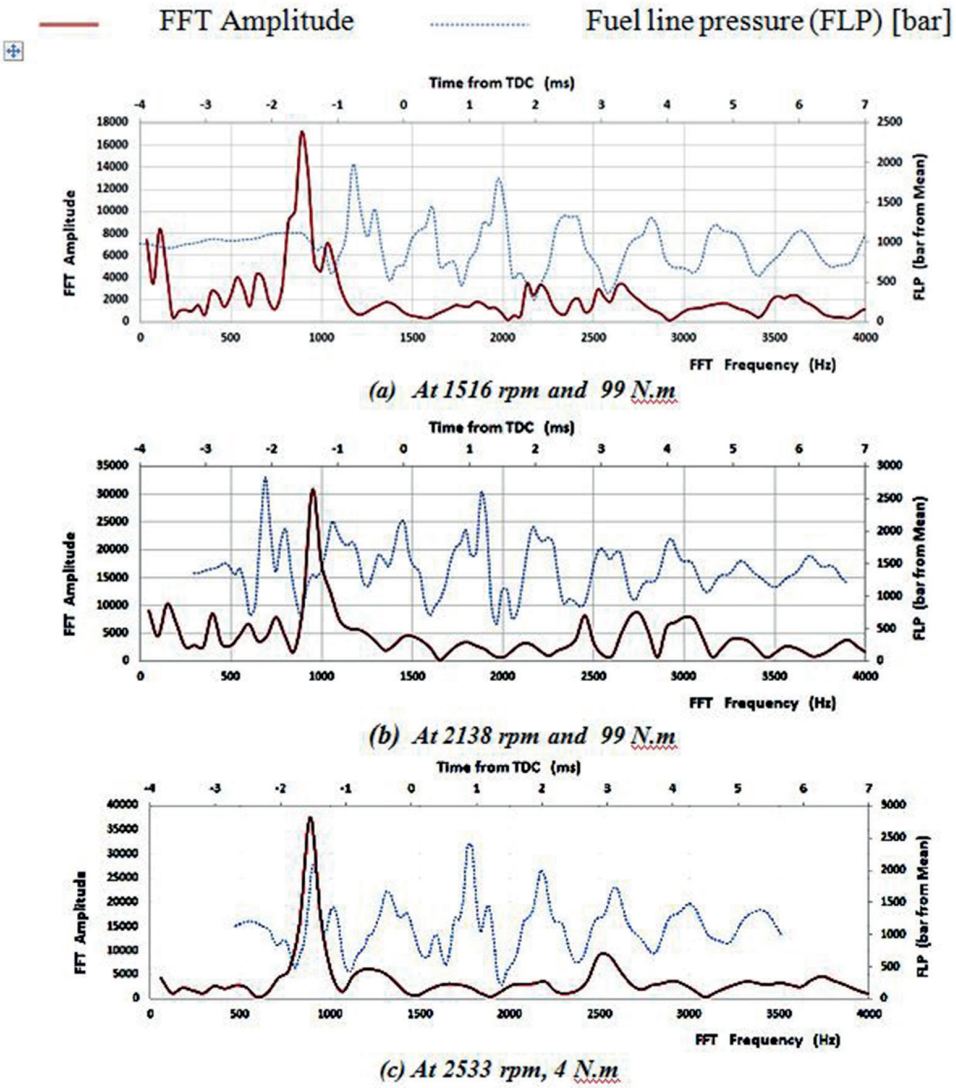

Figure 4 *Frequency analysis of the fuel line pressure*

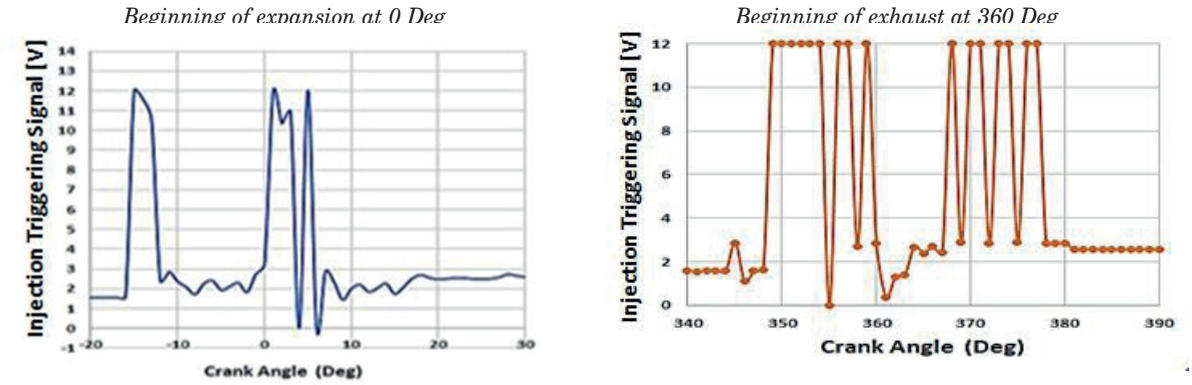

(a) Injection trigger signals at end of compression and beginning of expansion (Pilot and main Injections)

(b) Injection trigger signals at end of exhaust and beginning of suction (Preparation injections)

Figure 5 *The measured four trigger signals averaged over 42 successive cycles in crank angle scale at speed of 1527 rpm and load of 86 N.m*

Table 3 *The details of injector activation signals start, end and duration at engine speed of 1500 rpm and different loads (50, 100 and 150 N.m)*

	Pilot injection			Main injection		
	Start [ms]	End [ms]	Duration [ms]	Start [ms]	End [ms]	Duration [ms]
1500-50	-1.56	-1.26	0.3	-0.01	0.57	0.58
1500-100	-1.67	-1.26	0.41	-0.01	0.79	0.80
1500-150	-2.00	-1.26	0.74	0.41	1.28	0.87

Table 4 *The details of injector activation signals start, end and duration at engine speed of 2500 rpm and different loads (50, 100 and 150 N.m)*

	Pilot injection			Main injection		
	Start [ms]	End [ms]	Duration [ms]	Start [ms]	End [ms]	Duration [ms]
2500-50	-2.49	-2.23	0.26	-0.10	0.34	0.44
2500-100	-2.56	-2.04	0.52	-0.14	0.43	0.57
2500-150	-3.01	-2.42	0.59	-0.42	0.31	0.73

stroke. This early injection is made to prepare the homogeneous air-fuel charge. The remaining fuel is injected close to the TDC to control the combustion phase and this portion controls the beginning and duration of combustion [43]. Figure 5 shows the measured four trigger signals and their timing in crank angle degrees averaged over 42 successive cycles at 1527 rpm and 86 N.m.

The first activation signal (pilot injection) each time lasts for a very short period, 0.3 to 0.75 ms depending on the engine speed and load. It is timely adjusted so that fuel is injected into the cylinder 1.5 to 3 ms just before the Top Dead Centre (TDC) at the end of the compression stroke.

The small amount of injected fuel triggers the combustion of the fuel already present in the charge. Nearly 1 to 2 ms later, the injector is triggered again (main injection) for a period of nearly 0.4 to 0.9 ms. The fuel-injected in this case, at high pressure, initiates the main wave of combustion. The details of injector activation signals start, end and duration are presented in Tables 3 and 4 for speeds of 1500 and 2500 rpm respectively for three different loads.

The amount of fuel injected through any injection period is mainly a function of the injection pressure and injection period. The injector opening period is shown to increase with engine load at a constant speed to increase the amount of fuel injected as the injection pressure does not change marginally with engine load as shown in Figure 3 b. On the other hand, the injection duration is shown to decrease with the engine speed but the dramatic rise of injection pressure with speed (shown in Figure 3 a) compensates for this decrease and finally, the amount of fuel injected also increases with engine speed.

Two more short injections (1st and 2nd preparations) signals are timed just before the end of the exhaust stroke and just after the start of the suction stroke. These two injections control the preparation of the fresh homogenous charge for the next cycle. The 1st preparation signal is timely adjusted so that fuel is injected into the cylinder 1.5 ms just before the Top Dead Centre (TDC) at the end of the exhaust stroke. It ends almost at the end

of the exhaust stroke then the injector is triggered again (2nd preparation signal) for a period of another 1.5 ms. The period between the end of the 1st preparation and the start of the second preparation signal is about 1 ms. The numerical data about the four injections at different engine speeds and loads is introduced and utilized in numerical simulation of the multi-injection common rail injection system in [44].

It is noticed that the pilot and main injections are smooth and continuous. However, the trigger signals before and after the TDC before the suction stroke, consist of multiples of very short successive triggers. Short pulse widths are used enhance the evaporation and fuel-air mixing [30].

3.3 Cylinder pressure, AHRR and fuel-burning rate

Two approaches, heat-release rate and fuel mass burning rate can be used to acquire combustion information from pressure data [45]. Both techniques assume a uniform temperature of cylinder contents during the combustion process. Assuming the cylinder charge as a single zone and using the ideal gas law and neglecting crevice volume, blow-by and fuel injection effects, the first law of thermodynamics may be reduced to:

$$\frac{d(mu)}{dt} = -p\frac{dv}{dt} + \frac{dQ}{dt} + h_f\frac{dm}{dt}. \quad (4)$$

Many approaches for AHRR calculation have been offered in literature but the most widely used is that developed by Krieger and Borman [46]. The model is based on a polynomial fitting constant to compute the specific heat ratio c_p/c_v as a function of crank angle. This model was reported to strive for accuracy in representing the thermodynamic properties of the in-cylinder charge and involve substantial computations [47] and [48].

According to the sensitivity study for the significant variables carried by Krieger and Borman [49], the dissociation of the in-cylinder gases was ignored then u and R can be treated as constants, which allow for more simplifications. Following the steps explained in detail in Bosila [50], the Fuel-Burning Rate is calculated from the Equation 5:

$$\frac{dm}{dt} = \frac{[1+(c_v/R)]p\frac{dV}{dt} + \left(\frac{c_v}{R}\right)v\frac{dp}{dt} - (dQ/dt)}{h_f + (c_v/R)(pV/m) - u - D\left(\frac{\partial u}{\partial \varphi}\right)}, \quad (5)$$

$$D = \frac{m(1+f_o)}{m_0(f_s)}, \quad (6)$$

where: m - Mass of cylinder contents (kg),
u - Specific internal energy of the combustible mixture (kJ/kg),
p - Instantaneous cylinder pressure (N/m²),
V - Instantaneous cylinder volume (m³),
Q - The heat transfer to the gas within the combustion chamber,
h_f - Fuel specific enthalpy (kJ/kg),
f - Instantaneous equivalence ratio,
T - Instantaneous temperature of the charge inside the cylinder, which calculated from ideal gas equation,
R - The charge gas constant; $R(p, T, \varphi)$ calculated from correlation [50],
the subscript o denotes the initial value before fuel,
the subscript s denotes the stoichiometric value.

The AHRR is computed by multiplying the premeditated fuel burning rate by the fuel heating value. However, the associated AHRR uncertainty is calculated only for the fuel burning rate. Heywood [45] and Petitpas et al. [51] concluded that the uncertainty of AHRR is mostly due to the uncertainty of $\frac{dp}{dt}$, which is calculated from Equation (7)

$$U\left(\frac{dp}{d\varphi}\right) = \frac{\sqrt{(U^2(p_i) + U^2(pj))^2 + 2\left(\frac{P_j - P_i}{J-i}\right)^2 U^2(\varphi_j)}}{j-i}. \quad (7)$$

Calculations derived from Equation (7) result in max. uncertainty of $\frac{dp}{dt}$ is ±3.27%.

Figure 6 shows an example of the calculated charge temperature and the AHRR at the engine speed of

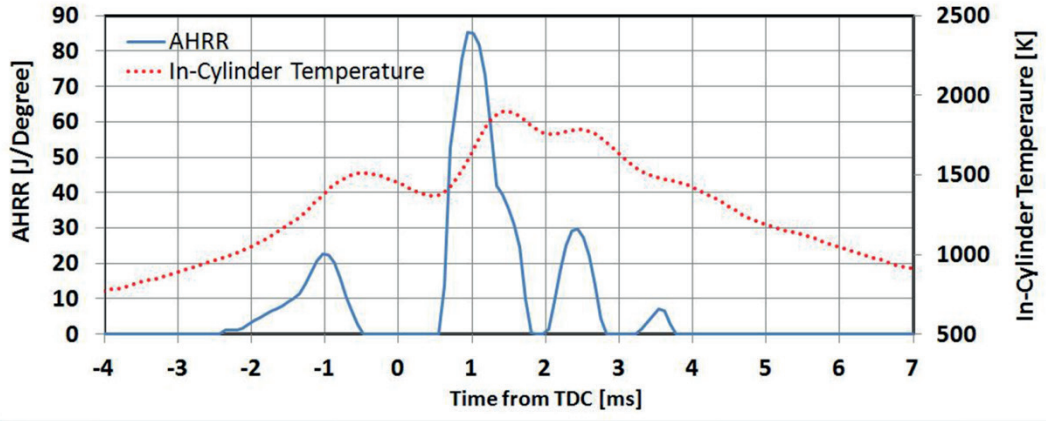

Figure 6 *Calculated AHHR and in-cylinder temperature at 2068 rpm and brake load of 200 Nm*

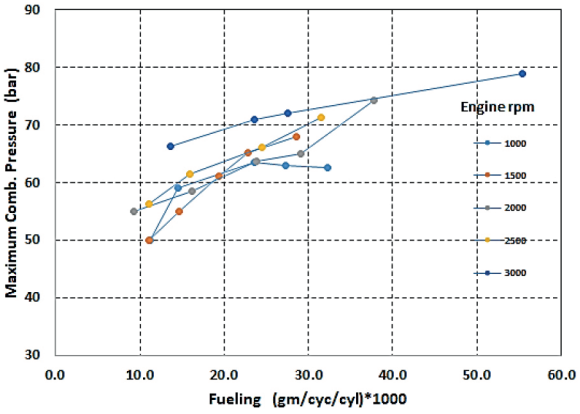

Figure 7 *Maximum measured combustion pressure*

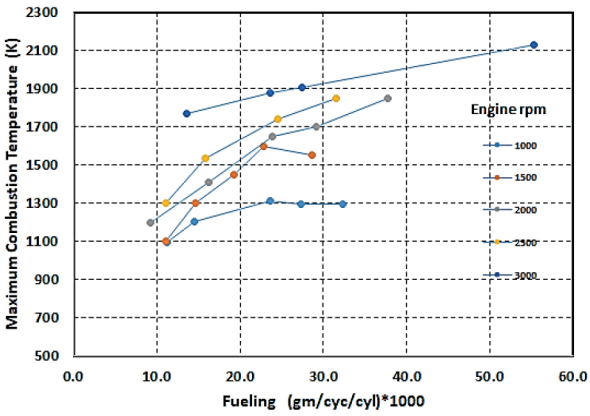

Figure 8 *Maximum calculated combustion temperature*

2068 rpm and a brake load of 200 N.m. It is seen that heat is released in waves (4 in this case). The number of burning waves, however, is not the same in all the cases, but changes with engine speed and brake load as will be explained in section 3.4. This means that in the HCCI engine the HRR curve is spread over a higher crank angle range, which decreases the maximum cycle pressure and temperature. In the case of the conventional diesel engine with similar specification [52], the peak heat release rate is about 220 J/degree in a single HR, whereas, in multiple injection HCCI, it is about (80-90) J/degree in high-temperature reaction (HTR) and (15-30) in low-temperature reaction (LTR).

Chen [53] analyzed the maximum in-cylinder pressure by considering that the peak cylinder pressure p_{max} is composed of the intake manifold air pressure p_{in} and two pressure rises from p_{in}; the pressure rise p_{maxp} due to the cylinder content compression/expansion without combustion; and the pressure rise p_{maxq} due to combustion and heat added to the cylinder content, which also undergoes compression/expansion thereafter toward p_{max}. The polytropic index plays a key role in the prediction of the pressure during the compression stroke [54]. It is affected by the polytropic exponent of compression, which decreases in HCCI engines due to the injection of an amount of fuel into the cylinder before compression. In addition, the thermal conductivity of the mixture increases with the amount of injected fuel [55]. The heat transfer between gases and the wall will increase. This suggested that P_{maxp} will decrease in HCCI engines than that of conventional engines. Concerning the pressure rise p_{maxq} due to the combustion added to the cylinder content, it was shown previously that the maximum heat release rate in HCCI engines is much lower than that of conventional engines and the HRR curve of HCCI engines is spread over a higher crank angle range. This results in lower maximum in-cylinder pressure. However, relatively higher pressure, compared to the conventional engine combustion, presents over a wide crank angle range.

The recorded cylinder pressure exhibited the maximum values shown in Figure 7, at different loads and speeds. It is observed that all the values are lower by nearly 7% compared to similar engines with traditional fuel injection systems [56]. Maximum temperatures, at different operating conditions, evaluated from thermodynamic relations during heat release calculations are also plotted in Figure 8. This would result in lower NO_x emission, not recorded in this work, especially at part load. Such observation was reported in previous publications [36, 57-58], which ,however, mentioned that CO percentage in the exhaust gases slightly increases. This was attributed to the expected incomplete combustion especially at high loads when little excess air is available.

3.4 Mutual effect between injection and combustion parameters

The measured in-cylinder, fuel line pressures and the injector trigger signal are plotted during the combustion period at 3 different speeds and loads, Figures 9 to 11. The calculated charge temperature and the AHRR are shown in the figure in each case.

It can be seen that the pilot injection trigger signal is advanced as engine speed increases (typically 1.5 to 3 ms before TDC). This is typical, because the delay period (approximately 1 to 1.5 ms), increases in terms of crank angle and the combustion is planned to start nearly 1 ms or less before TDC.

The second (main) injection trigger signal starts after nearly 1.5 to 2 ms followed by a shorter delay (typically 0.7 to 1 ms) before the main combustion wave commences. The delay period of the main injection is shorter than that of the pilot injection due to the higher temperature attained during the main injection than that in the pilot injection due to the heat released during the low-temperature reaction. The temperature curve at each operating condition is shown to increase more steeply in the periods of the low and high-temperature reactions (Consistent with pressure and HRR curves) and decreases in the period between the low and high temperatures reactions.

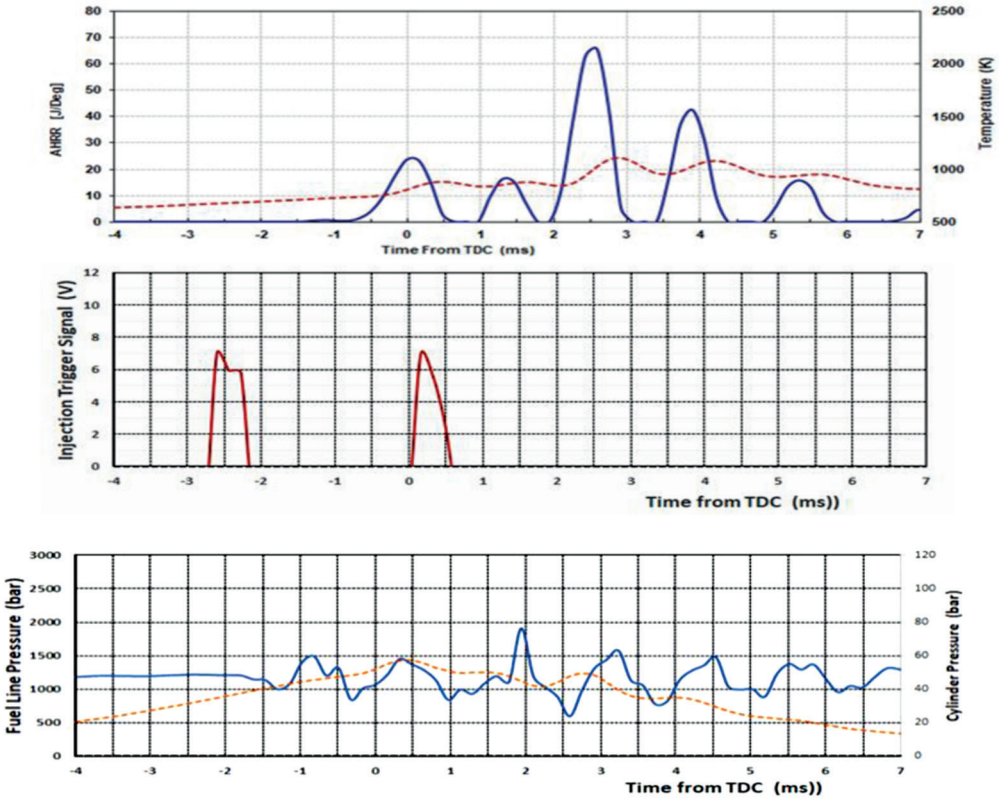

Figure 9 *AHRR, cylinder temperature, injector signal, fuel line and cylinder pressures at RPM=1027, brake load = 14 Nm*

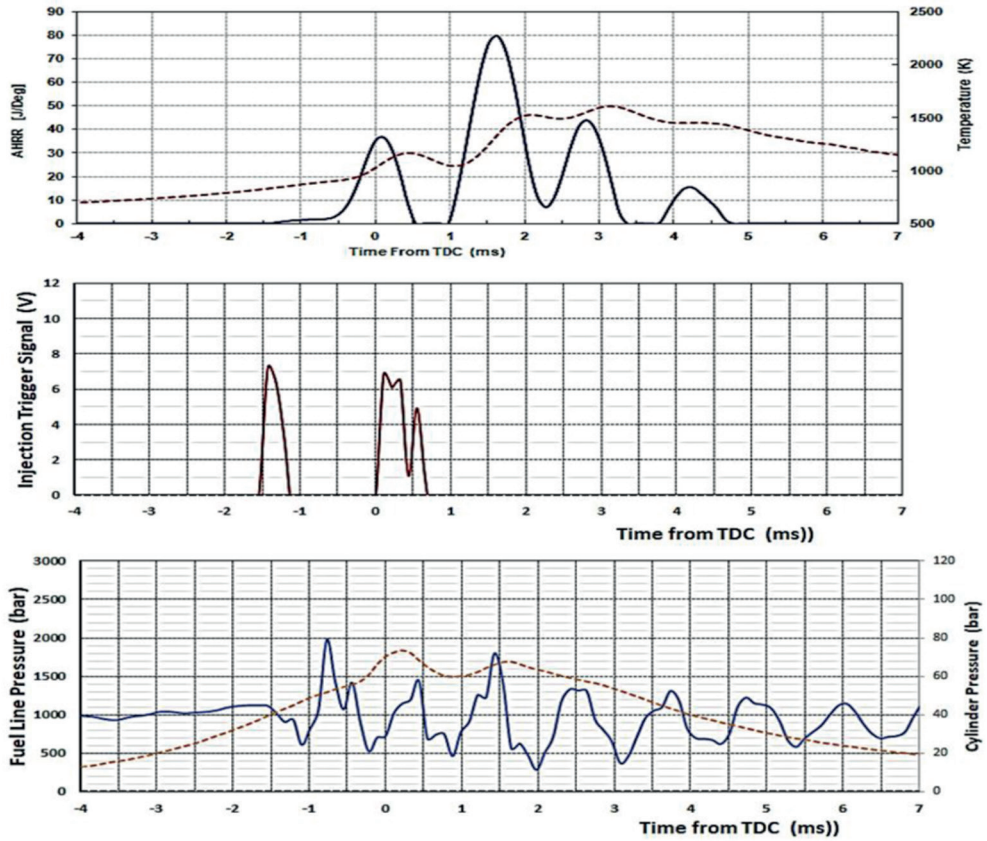

Figure 10 *AHRR, cylinder temperature, injector signal, fuel line and cylinder pressures at RPM=1516, brake load = 99 Nm*

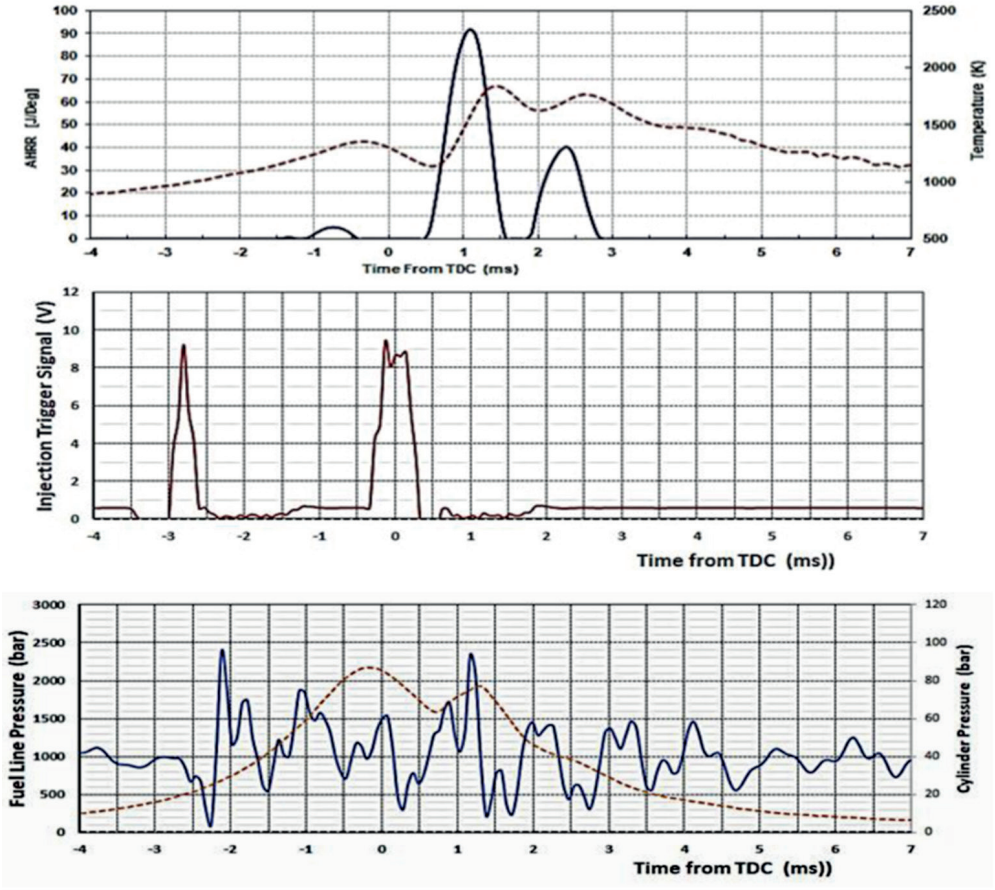

Figure 11 *AHRR, cylinder temperature, injector signal, fuel line and cylinder pressures at RPM=2531, brake load = 141 Nm*

The early charge preparation method results in improved mixture homogeneity compared to other methods. Two stages of combustion are identified for HCCI engines due to the low and high-temperature chemical kinetics of diesel fuel. So more than one peak are noticed on the pressure history diagram. These peaks are due to the multiple heat release rate attained during combustion as shown in Figure 9.

At low brake loads, (Figure 9) too much air is present in the combustible mixture. This decreases the flame front travel speed, which results in a low rate of temperature rise. Single-zone modelling suggested a smallest temperature threshold of 1400 to 1500 K for the in-cylinder temperature for complete combustion before expansion [7]. Consequently, a considerable portion of the fuel present in the fresh charge remains un-burnt after the second wave of combustion. This portion burns as it reaches the self-ignition, which can happen in several instances causing more waves of combustion, especially at lower engine speeds.

As the engine speed and load increase, the injection pressure and durations increase and consequently, the injected fuel rate increases at each split injection [58-59]. This may explain the higher value of maximum heat released at higher engine speed and load.

The combustion waves cause the cylinder pressure to simultaneously increase over the polytropic expansion usually experienced with traditional injection systems. The combustion, therefore, is spread over a long duration while the piston is moving down away from the TDC.

The pressure waves in the fuel line pressure are initiated at the moment at which the injector starts to open. This instant follows the first injection trigger signal by almost 0.5 ms at speeds of 1516 and 2531 rpm while it was about 1 ms at speed of 1027 rpm. The main injection trigger signal is also followed by the second pressure wave, which adds to the previous one. The resulting net pressure variation pattern seems to happen invariably at all speeds and loads with minor effects of further heat release waves.

4 Conclusions

The injection and combustion parameters of an HCCI Diesel engine with a Common Rail direct fuel injection system are experimentally investigated. Measured injector activation signal suggested that the fresh charge is internally prepared by injecting fuel twice, just before and then after the Top Dead Center before the suction stroke. Combustion is triggered by a pilot injection, 1.5 to 3 milliseconds (ms) before the Top Dead Center, followed by a secondary (main) injection, typically starting at the top dead center.

- The mean value of the fuel line pressure is found to increase with engine speed and marginally with the load. Typical mean values are 700 bar at 1000 rpm and increases almost linearly with speed to nearly 1600 bar at 3000 rpm.
- The pilot and main injector trigger signals are found smooth and continuous. However, the trigger signals before and after the TDC before the suction stroke, consist of multiples of very short successive triggers. The variations in the signal pattern from cycle to cycle are also very small. It is difficult, however, to determine the amount of fuel injected during these two periods.
- The Fuel Burning Rate is calculated and reported at different operating conditions. It is seen that the heat is released in waves depending on the engine speed and load. The number of burning waves increases with the decrease of engine speed and load. The pilot injection trigger signal timing is typically 1.5 to 3 ms before TDC and the first combustion wave starts nearly 1 to 1.5 ms later. The second (main) injection signal timing is nearly 1 to 2 ms after the first and is followed by a typical delay of 0.7 to 1 ms after which the second wave of combustion commences. At low brake loads, however, more waves of combustion are observed especially at low speeds. This is attributed to the lower equivalence ratio and low charge temperature and consequently lower flame speed.
- The maximum value of heat release wave increases with the increase of engine speed and load due to the increase of injection pressure and durations. Consequently, the mass of fuel injected.
- Pressure waves in the fuel line pressure are initiated almost 0.5 ms after the pilot injection trigger signal. The main injection trigger signal is also followed by the second pressure wave, which adds to the previous one. The resulting net pressure variation pattern seems to happen invariably at all speeds and loads and even at all injector fuel lines. The FFT transform of the fuel line pressure signal shows that the major frequency of the signal is nearly the same, 850 to 950 Hz. Calculating the period of pressure wave travel from the pipe length and fuel Bulk's modulus confirms the measured frequency based on pipe length of 0.395 m and free-closed boundary condition.
- The maximum cycle values of measured cylinder pressure and calculated temperature are presented at different loads and speeds. It is observed that all values are lower by nearly 7% compared to similar engines with a traditional fuel injection system. Thus, the lower NOx emission, not measured in this work, especially at part loads is to be expected.

The presented experimental measurements results and conclusions could be very useful for developing simulation models that help in engine assessment, modeling, control, emission reduction and power saving. However, further investigations are needed to assess the practical response of the fuel injector to each trigger signal. This is necessary to evaluate the amount of fuel injected at each stage and the homogeneous charge characteristics. More work is needed to develop a fuel-burning rate model for engine simulation programs, that suit the conditions of combustion in such charge.

Acknowledgment

The authors greatly appreciate the assistance of the Military Technical College in Egypt especially the department of mechanical power and energy.

References

[1] ZHAO, H. Outlook and future directions in HCCI/CAI engines. In: *HCCI and CAI engines for the automotive industry*. ZHAO, H. (ed.). 1. ed. Cambridge England: Woodhead Publishing in Mechanical Engineering. 2007. eISBN 9781845693541.

[2] STANGLMAIER, R. H., ROBERTS, C. E. Homogeneous charge compression ignition (HCCI): benefits, compromises and future engine applications. *SAE Technical Paper* [online]. 1999, 1999-01-3682. ISSN 0148-7191, eISSN 2688-3627. Available from: https://doi.org/10.4271/1999-01-3682

[3] SCHLEPPE, M. N. SI - HCCI mode switching optimization using a physics based model [online]. MSc thesis. Edmonton, Alberta: Department of Mechanical Engineering, 2011. Available from: https://doi.org/10.7939/R38K9M

[4] SUZUKI T, KAKEGAWA, T, HIKINO, K. Development of diesel combustion for commercial vehicles. *SAE Technical Paper* [online]. 1997, 972685. ISSN 0148-7191, eISSN 2688-3627. Available from: https://doi.org/10.4271/972685

[5] CATANIA, A. E., FERRARI, A., MANNO, M., SPESSA, E. Experimental investigation of dynamics effects on multiple-injection common rail system performance. *Journal of Engineering for Gas Turbines and Power* [online]. 2008, **130**, p. 1-13. ISSN 0742-4795, eISSN 1528-8919. Available from: https://doi.org/10.1115/1.2835353

[6] DEC, J. E., SJOBERG, M. Isolating the effects of fuel chemistry on combustion phasing in an HCCI engine and the potential of fuel stratification for ignition control. *SAE Technical Paper* [online]. 2004, 2004-01-0557. ISSN 0148-7191, eISSN 2688-3627. Available from: https://doi.org/10.4271/2004-01-0557

[7] SJOBERG, M., DEC, J. E. Combined effects of fuel-type and engine speed on intake temperature requirements and completeness of bulk-gas reactions for HCCI combustion *SAE Technical Paper* [online]. 2003, 2003-01-3173. ISSN 0148-7191, eISSN 2688-3627. Available from: https://doi.org/10.4271/2003-01-3173

[8] KELLY-ZION, P. L., DEC, J. E. A computational study of the effect of fuel type on ignition time in homogeneous charge compression ignition engines. *Proceedings of the Combustion Institute* [online]. 2000, **28**(1), p. 1187-1194. ISSN 1540-7489. Available from: https://doi.org/10.1016/S0082-0784(00)80329-X

[9] MULEMANE, A., HAN, J., LU, P., YOON, S., LAI, M. Modeling dynamic behavior of diesel fuel injection systems. *SAE Technical Paper* [online]. 2004, 2004-01-0536. ISSN 0148-7191, eISSN 2688-3627. Available from: https://doi.org/10.4271/2004-01-0536

[10] UBERTINI, S. Injection pressure fluctuations model applied to a multi-dimensional code for diesel engines simulation. In: 7th Biennial Conference on Engineering Systems Design and Analysis ESDA04: proceedings. 2004. p. 1-9.

[11] HERFATMANESH, M. R., PENG, Z., IHRACSKA, A., LIN, Y., LU, L., ZHANG, C. Characteristics of pressure wave in common rail fuel injection system of high-speed direct injection diesel engines. *Advances in Mechanical Engineering* [online]. 2016, **8**, p. 1-8. ISSN 1687-8140, eISSN 1687-8140. Available from: https://doi.org/10.1177/1687814016648246

[12] GAMBRILL, R. The sensitivity of diesel engine performance to fuel injection parameters at various operating points. PhD thesis. Nottingham: University of Nottingham, 2004.

[13] CATANIA, A. E., FERRARI, A., MITTICA, A., SPESSA, E., TORINO, P. Common rail without accumulator: development, theoretical-experimental analysis and performance enhancement at DI-HCCI level of a new generation FIS. *SAE Technical Paper* [online]. 2007, 2007-01-1258. ISSN 0148-7191, eISSN 2688-3627. Available from: https://doi.org/10.4271/2007-01-1258

[14] ZHAO J, WANG J. On-board fuel property identification method based on common rail pressure signal. In: ASME 2012 5th Annual Dynamic Systems Control Conference Joint with JSME 2012 11th Motion and Vibration Conference: proceedings. 2012.

[15] HAYAT, Q., LIYUN, F., SONG, E., XIUZHEN, M., BINGQI, T., FAROUK, N. Study of effect of diesel fuel properties on pressure wave profile. *Applied Mechanics and Materials* [online]. 2014, **681**, p. 19-22. ISSN 1662-7482. Available from: https://doi.org/10.4028/www.scientific.net/AMM.681.19

[16] HENEIN, N. A., LAI, M., SINGH, I. P., ZHONG, L., HAN, J. Characteristics of a common rail diesel injection system under pilot and post injection modes. *SAE Technical Paper* [online]. 2002, 2002-01-0218. ISSN 0148-7191, eISSN 2688-3627. Available from: https://doi.org/10.4271/2002-01-0218

[17] BAUMANN, J., KIENCKE, U., SCHLEGL, T., OESTREICHER, W. Practical feasibility of measuring pressure waves in common rail injection systems by magneto-elastic sensors. *SAE Technical Paper* [online]. 2006, 2006-01-0891. ISSN 0148-7191, eISSN 2688-3627. Available from: https://doi.org/10.4271/2002-01-0218

[18] LI, P., ZHANG, Y., LI, T., XIE, L. Elimination of fuel pressure fluctuation and multi-injection fuel mass deviation of high pressure common-rail fuel injection system. *Chinese Journal of Mechanical Engineering* [online]. 2015, **28**, p. 294-306. ISSN 1000-9345, eISSN 2192-8258. Available from: https://doi.org/10.3901/CJME.2014.1216.180

[19] YIHUI, C., GUANGYAO, O., HAILONG, C., JINGQIU, Z. Research on the eliminating of pressure oscillation for augment common-rail injection system. In: 2011 IEEE 2nd International Conference on Computing, Control and Industrial Engineering CCIE 2011: proceedings. 2011. p. 6-9.

[20] KUMAR, V., ZHANG, Z., SUN, Z. Modeling and control of a novel pressure regulation mechanism for common rail fuel injection systems. *Applied Mathematical Modelling* [online]. 2011, **35**(7), p. 3473-3483. ISSN 0307-904X. Available from: https://doi.org/10.1016/j.apm.2011.01.008

[21] TIAN, B., FAN, L., MA, X., WANG, H., LIU, H. Study of fuel injection quantity fluctuation in high pressure common rail system in entire operating conditions. *Advanced Materials Research* [online]. 2012, **562-564**, p. 1048-1053. ISSN 1662-8985. Available from: https://doi.org/10.4028/www.scientific.net/AMR.562-564.1048

[22] BINGQI, T., LIYUN, F., XIUZHEN, M., HAYAT, Q., YUN, B., YANG, L. Investigation of main injection quantity fluctuation due to pilot injection in high pressure common rail fuel injection system. *International Journal on Smart Sensing and Intelligent Systems* [online]. 2014, **7**(2), p. 820-836. eISSN 1178-5608. Available from: https://doi.org/10.21307/ijssis-2017-683

[23] YU, W., YANG, W., MOHAN, B., TAY, K., ZHAO, F. Multiple injections study based on an advanced combustion investigation system. *Energy Procedia* [online]. 2015, **75**, p. 900-905. ISSN 1876-6102. Available from: https://doi.org/10.1016/j.egypro.2015.07.222

[24] AGARWAL, A. K., SINGH, A. P., MAURYA, R. K. Evolution, challenges and path forward for low temperature combustion engines. *Progress in Energy and Combustion Science* [online]. 2017, **61**, p. 1-56. ISSN 0360-1285. Available from: https://doi.org/10.1016/j.pecs.2017.02.001

[25] AGARWAL, A. K., SINGH, A. P., MAURYA, R. K., SHUKLA, P. C., DHAR, A., SRIVASTAVA, D. K. Combustion characteristics of a common rail direct injection engine using different fuel injection strategies.

International Journal of Thermal Sciences [online]. 2018, **134**, p. 475-484. ISSN 1290-0729. Available from: https://doi.org/10.1016/j.ijthermalsci.2018.07.001

[26] XU, L., BAI, X.-S., JIA, M., QIAN, Y., QIAO, X., LU, X. Experimental and modeling study of liquid fuel injection and combustion in diesel engines with a common rail injection system. *Applied Energy* [online]. 2018, **230**, p. 287-304. ISSN 0306-2619. Available from: https://doi.org/10.1016/j.apenergy.2018.08.104

[27] LIU, E., WANHUA, S. U. Study on effects of common rail injector drive circuitry with different freewheeling circuits on control performance and cycle-by-cycle variations. *Energies* [online]. 2019, **12**(3), 564. eISSN 1996-1073. Available from: https://doi.org/10.3390/en12030564

[28] HELMANTEL, A., DENBRATT, I. HCCI operation of a passenger car common rail DI diesel engine with early injection of conventional diesel fuel. *SAE Technical Paper* [online]. 2004, 2004-01-0935. ISSN 0148-7191, eISSN 2688-3627. Available from: https://doi.org/10.4271/2004-01-0935

[29] BUCHWALD, R., BRAUER, M., BLECHSTEIN, A., SOMMER, A., KAHRSTEDT, J. Adaption of injection system parameters to homogeneous diesel combustion. *SAE Technical Paper* [online]. 2004, 2004-01-0936. ISSN 0148-7191, eISSN 2688-3627. Available from: https://doi.org/10.4271/2004-01-0936

[30] SU, W., ZHANG, X., LIN, T., PEI, Y., ZHAO, H. Study of pulse spray, heat release, emissions and efficiencies in a compound diesel HCCI combustion engine. In: Internal Combustion Engine Division Fall Technical Conference ASME 2004: proceedings [online]. 2004. ISBN 0-7918-3746-7, p. 389-398. Available from: https://doi.org/10.1115/ICEF2004-0927

[31] SU, W., WANG, H., LIU, B. Injection mode modulation for HCCI diesel combustion. *SAE Technical Paper* [online]. 2005, 2005-01-0117. ISSN 0148-7191, eISSN 2688-3627. Available from: https://doi.org/10.4271/2005-01-0117

[32] CATANIA, A. E., FERRARI, A., SPESSA, E. Numerical-experimental study and solutions to reduce the dwell-time threshold for fusion-free consecutive injections in a multijet solenoid-type cr system 1. *Journal of Engineering for Gas Turbines and Power* [online]. 2009, **131**, p. 1-14. ISSN 0742-4795, eISSN 1528-8919. Available from: https://doi.org/10.1115/1.2938394

[33] LAWLER, B., LACEY, J., GURALP, O., NAJT, P., FILIPI, Z. HCCI combustion with an actively controlled glow plug: The effects on heat release, thermal stratification, efficiency and emissions. *Applied Energy* [online]. 2018, **211**, p. 809-819. ISSN 0306-2619. Available from: https://doi.org/10.1016/j.apenergy.2017.11.089

[34] LAWLER, B., MAMALIS, S., JOSHI, S., LACEY, J., GURALP, O., NAJT, P., FILIPI, Z. Understanding the effect of operating conditions on thermal stratification and heat release in a homogeneous charge compression ignition engine. *Applied Thermal Engineering* [online]. 2017, **112**, p. 392-402. ISSN 1359-4311. Available from: https://doi.org/10.1016/j.applthermaleng.2016.10.056

[35] EBRAHIMI, R., DESMET, B. An experimental investigation on engine speed and cyclic dispersion in an HCCI engine. *Fuel* [online]. 2010, **89**(8), p. 2149-2156. ISSN 0016-2361. Available from: https://doi.org/10.1016/j.fuel.2010.04.005

[36] GOWTHAMAN, S., SATHIYAGNANAM, A. P. A review of homogeneous charge compression ignition (HCCI) engine. *International Journal of Scientific & Engineering Research*. 2015, **6**(1), 779. ISSN 2229-5518.

[37] IIDA, M., AROONSRISOPON, T., HAYASHI, M., FOSTER, D., MARTIN, J. The effect of intake air temperature, compression ratio and coolant temperature on the start of heat release in an HCCI (homogeneous charge compression ignition) engine. *SAE Technical Paper* [online]. 2001, 2001-01-1880/4278. ISSN 0148-7191, eISSN 2688-3627. Available from: https://doi.org/10.4271/2001-01-1880

[38] IIDA, M., HAYASHI, M., FOSTER, D. E., MARTIN, J. K. Characteristics of homogeneous charge compression ignition (HCCI) engine operation for variations in compression ratio, speed and intake temperature while using n-butane as a fuel. *Journal of Engineering for Gas Turbines and Power* [online]. 2003, **125**(2), p. 472-478. ISSN 0742-4795, eISSN 1528-8919. Available from: https://doi.org/10.1115/1.1501914

[39] MAURYA, R. K., AGARWAL, A. K. Experimental investigation on the effect of intake air temperature and air - fuel ratio on cycle-to-cycle variations of HCCI combustion and performance parameters. *Applied Energy* [online]. 2011, **88**, p. 1153-1163. ISSN 0306-2619. Available from: https://doi.org/10.1016/j.apenergy.2010.09.027

[40] FARMAAN, A. K. M., MUKUND, R., PRAKASH, S. A., PRADEEP, P., AROUL, V. A., SENTHIL, M. Experimental and computational investigation of engine characteristics in a compression ignition engine using mahua oil. *Fuel* [online]. 2021, **284**, 119007. ISSN 0016-2361. Available from: https://doi.org/10.1016/j.fuel.2020.119007

[41] NIKLAWY, W., SHAHIN, M., AMIN, M. I., ELMAIHY, A. Performance of homogeneous charge compression ignition (HCCI) engine with common rail fuel injection. *IOP Conference Series: Materials Science and Engineering* [online]. 2020, **973**, 012038. ISSN 1757-8981, eISSN 1757-899X. Available from: https://doi.org/10.1088/1757-899x/973/1/012038

[42] CATANIA, A. E., FERRARI, A., MITTICA, A. High-pressure rotary pump performance in multi-jet common rail systems. In: ASME 8th Biennial Conference on Engineering Systems Design and Analysis ESDA 2006: proceedings. 2006. p. 1-9.

[43] LIANG, X., ZHENG, Z., ZHANG, H., WANG, Y., HANZHENGNAN, Y. A review of early injection strategy in premixed combustion engines. *Applied Sciences* [online]. 2019, **9**(18), 3737. eISSN 2076-3417. Available from: https://doi.org/10.3390/app9183737

[44] NIKLAWY, W., SHAHIN, M., AMIN, M. I. Modelling and experimental investigation of high - pressure common rail diesel injection system. *IOP Conference Series: Materials Science and Engineering* [online]. 2020, **973**, 012037. ISSN 1757-8981, eISSN 1757-899X. Available from: https://doi.org/10.1088/1757-899X/973/1/012037

[45] HEYWOOD, J. B. *Internal combustion engine (ICE) fundamentals*. USA: McGraw-Hill, 1988. ISBN 0-07-028637-X.

[46] VAN GERPEN, J., REITZ, D. R. Diesel combustion and fuels. In: *Diesel engine reference book*. CHALLEN, B., BARANESCU, R. (eds.). London: Butterworth-Heinemann, 1984. ISBN 0-408-00443-6.

[47] GATOWSKI, J. A., BALLES, E. N., CHUN, K. M., NELSON, F. E., EKCHIAN, J. A., HEYWOOD, J. B. Heat release analysis of engine pressure data. *SAE Technical Paper* [online]. 1984. ISSN 0148-7191, eISSN 2688-3627. Available from: https://doi.org/10.4271/841359

[48] FATHI, M., SARAY, R. K., CHECKEL, M. D. Detailed approach for apparent heat release analysis in HCCI engines. *Fuel* [online]. 2010, **89**(9), p. 2323-2330. ISSN 0016-2361. Available from: https://doi.org/10.1016/j.fuel.2010.04.030

[49] KRIEGER, R. B., BORMAN, G. L. *The computation of apparent heat release for internal combustion engines*. ASME 66-WA/DGP-4. New York, N.Y: ASME, 1966.

[50] BOSILA, A. Cyclic variation for spark ignition engines using natural gas. PhD. thesis. Department of Mechanical Power and Energy, Military Technical College, 2010.

[51] PETITPAS, G., MCNENLY, M. J., WHITESIDES, R. A., LIVERMORE, L. A framework for quantifying measurement uncertainties and uncertainty propagation in HCCI / LTGC engine experiments. *SAE International Journal of Engines* [online]. 2017, **10**(3), p. 1275-1296. ISSN 1946-3936, e-ISSN 1946-3944. Available from: https://doi.org/10.4271/2017-01-0736

[52] MATHIVANAN, K., MALLIKARJUNA, J. M., RAMESH, A. Influence of multiple fuel injection strategies on performance and combustion characteristics of a diesel fueled HCCI engine - an experimental investigation. *Experimental Thermal and Fluid Science* [online]. 2016, **77**, p. 337-346. ISSN 0894-1777. Available from: https://doi.org/10.1016/j.expthermflusci.2016.05.010

[53] CHEN, G. Prediction of peak cylinder pressure variations over varying inlet air condition of compression-ignition engine. *Engineering for Gas Turbines and Power* [online]. 2007, **129**, p. 589-595. ISSN 0742-4795, eISSN 1528-8919. Available from: https://doi.org/10.1115/1.2431389

[54] LEE, Y., MIN, K. Estimation of the polytropic index for in-cylinder pressure prediction in engines. *Applied Thermal Engineering* [online]. 2019, **158**, 113703. ISSN 1359-4311. Available from: https://doi.org/10.1016/j.applthermaleng.2019.04.113

[55] LUO, Q., SUN, B., TIAN, H. The characteristic of polytropic coefficient of compression stroke in hydrogen internal combustion engine. *International Journal of Hydrogen Energy* [online]. 2014, **39**(25), p. 13787-13792. ISSN 0360-3199. Available from: https://doi.org/10.1016/j.ijhydene.2014.04.035

[56] MAE, F. Diesel engine turbocharger match, evaluation and improvement. PhD. thesis. Department of Mechanical Power and Energy, Military Technical College 1995.

[57] TANAKA, S., AYALA, F., KECK, J. C. A reduced chemical kinetic model for HCCI combustion of primary reference fuels in a rapid compression machine. *Combustion and Flame* [online]. 2003, **133**(4), p. 467-481. ISSN 0010-2180. Available from: https://doi.org/10.1016/S0010-2180(03)00057-9

[58] WANG, Z., WYSZYNSKI, M. L., XU, H., ROSLI, N., PIASZYK, J. Fuel injection and combustion study by the combination of mass flow rate and heat release rate with single and multiple injection strategies. *Fuel Processing Technology* [online]. 2015, **132**, p. 118-132. ISSN 0378-3820. Available from: https://doi.org/10.1016/j.fuproc.2014.11.024

[59] WANG, Z., DING, H., WYSZYNSKI, M. L., TIAN, J., XU, H. Experimental study on diesel fuel injection characteristics under cold start conditions with single and split injection strategies. *Fuel Processing Technology* [online]. 2015, **131**, p. 213-222. ISSN 0378-3820. Available from: https://doi.org/10.1016/j.fuproc.2014.10.003